한국기계가공학회지, 제20권, 제10호, pp. 119~127(2021.10) ISSN 1598-6721(Print)
Journal of the Korean Society of Manufacturing Process Engineers, Vol. 20, No. 10, pp. 119~127(2021.10) ISSN 2288-0771(Online)

https://doi.org/10.14775/ksmpe.2021.20.10.119

Determining Factors to Enhanced Oil Mist Filter Efficiency Using CFD Modeling

Hee-Jae Shin*,#

*Department of Mechanical Engineering, VISION College of Jeonju.

CFD모델링을 통한 오일 미스트필터효율 향상 결정요소에 관한 연구

신희재*,#

*전주비전대학교 기계과

(Received 17 September 2021; received in revised form 21 September 2021; accepted 29 September 2021)

ABSTRACT

Small drops in gas cause some problems for downstream equipments such as turbine, compressor and etc. In some cases, we are obliged to remove hazardous liquid mist from gas. In order to remove water or other liquids from the gas, there are some equipments like mesh mist eliminator and vane-plate mist eliminator. oil mist filter is a kind of liquid eliminator equipments used to remove the liquid with 1-10um droplet diameter from the gas. In this paper is determine the factors affecting the oil mist filter efficiency using CFD. length and angle of the filter were considered and the results and compare the results of the efficiency tests, showed error of less than 3%. optimum filter can remove more than 87.3% between 1 and 10um of oil mist.

Keywords : Over the Range(OTR)(후드겸용 전자레인지), Oil Mist Filter(오일미스트필터), Computational Fluid Dynamics(CFD)(전산유체역학)

1. Introduction

It is a trend to use Over the Range (OTR) on household gas oven with microwave hood combination in electronics companies recently. that is the process of cooking food in the oven using the heat from the gas oven[1-5]. However, harmful gases that occur in the process of cooking variety of foods in the kitchen as well as the surrounding environment can have a bad impact on the human such as respiratory disease and lung disease, asthma, atopic dermatitis, respiratory disorders, nervous system disorders[3,6-8]. Therefore OTR for the filter that can block harmful gases is required by the situation. That is currently being used in the form of a Mesh Filter consists of mesh geometry, the removal efficiency of the Oil Mist Filter to appear very low, there is a problem[1]. Therefore it is priority to have a higher removal efficiency of the Oil mist Filter than existing

Corresponding Author : ostrich@jj.ac.kr
Tel: +82-63-220-4073, Fax: +82-63-220-4079

Mesh Filter.

Existing research on OTR has focused on improving the performance of OTR and filter research was almost nonexistent. Jeon W. H studied the characteristics of the noise of the OTR sirocco fan, seized the noise characteristics of OTR and investigated in the development of a low-noise fan based on the numerical analysis and experiment[9]. Y. I. Shin mainly studied the changing of ventilation of a motor and hood for OTR to improve high-capacity, cooking space and performance[5]. J. Gharib studied trapping efficiency through the theory of numerical analysis and CFD interpretation to identify performance of filter[2]. Lee studied a performance of trapping efficiency and pressure drop through the optical design about a shape of Filter to remove big mist that is larger than 1mm.

In this study, to maximize the efficiency of the Filter and Filter pressure drop can be minimized by design using ANSYS Fluent 13.0 which is computational fluid dynamics analysis program that performs the analysis and select the optimal model to produce the product, develop with high removal efficiency and low pressure drop in the Oil Mist Filter Efficiency Test and develop high-performance Filter through a comparison with existing products[4,10].

2. Materials and Methods

In order to perform analysis, four assumptions are defined. 1) Droplets are assumed as spheres. 2) There's no interaction between liquid-liquid. 3) There's no re-entrainment of the trapped liquid. 4) The only acting force is drag. 5) 2-D Analysis due to the same feature in the width direction[2].

The water volume fraction is 0.09, so it satisfies the fundamental assumption that mentions the dispersed second phase occupies a low volume fraction. In Eulerian-Lagrangian model the continuum phase is fluid phase and it is solved by Navier-Stokes equations, while the dispersed phase is solved by tracking the droplets through the flow field. The dispersed phase exchanges momentum and energy with the fluid phase[2,11].

2.1 Droplet motion equation

The motion of a single particle of arbitrary density is governed by the following equations[2,12-14].

$$\frac{d\vec{u_d}}{d_t} = \frac{\vec{u_g} - \vec{u_d}}{\tau_d} \tag{1}$$

u_g: the gas velocity, u_d: the droplet velocity.

τ_d: the droplet relaxation time.

τ_d is calculated as follows;

$$\tau_d = \frac{4\rho_d d_p}{3\rho_g c_d \left|\vec{u_g} - \vec{u_d}\right|} \tag{2}$$

C_d is calculated according to Schiller-Naumann;

$$C_d = \frac{24}{Re_d}(1 + 0.15 Re_d^{0.687}) \tag{3}$$

Drag coefficient is function of Re number of droplet. Re number is defined as follows;

$$Re = \frac{pd\left|u_p - u\right|}{\mu} \tag{4}$$

The variables needed for the solver are: gas densities, droplet diameter, volume fraction of liquid (BIS PHTHALATE), mean gas velocity, Reynolds number.

$$\frac{du_p}{dt} = F_D(u - u_p) + \frac{g_x\left|\rho_p - \rho\right|}{\rho_p} + F_x \tag{5}$$

where u_p: the particle velocity, u: the flow velocity, ρ: the fluid density. F_x: additional acceleration, F_d: drag force, ρ_p: the particle density.

F_D is the drag force per unit particle mass and can be obtained from;

$$F_D = \frac{18\mu}{\rho_p d_p^2}\frac{C_D Re}{24} \tag{6}$$

2.2 Continuous phase model

Standard k-ε is reasonable accurate and it is a semi-empirical model, so that the equation derivation relies on phenomenological considerations and empiricism. This model is applicable to wall-bounded flows. The turbulence kinetic energy k, and its rate of dissipation ε, are obtained from the following k-ε Transport Equations[15-16].

$$\frac{\partial}{\partial t}(\rho k)+\frac{\partial}{\partial x_j}(\rho k u_j) = \frac{\partial}{\partial x_j}\left[(\mu+\frac{\mu_t}{\sigma_k})\frac{\partial k}{\partial x_j}\right]+\mu\frac{\partial u_i}{\partial x_j}\left[\frac{\partial u_i}{\partial x_j}+\frac{\partial u_j}{\partial x_i}\right]-\rho\epsilon \quad (7)$$

$$\frac{\partial}{\partial t}(\rho\epsilon)+\frac{\partial}{\partial x_k}(\rho k u_k) = \frac{\partial}{\partial x_k}\left[(\mu+\frac{\mu_t}{\sigma_\epsilon})\frac{\partial \epsilon}{\partial x_k}\right] + \frac{C_1\epsilon}{k}\mu\frac{\partial u_i}{\partial x_j}\left[\frac{\partial u_i}{\partial x_j}+\frac{\partial u_j}{\partial x_i}\right]-C_{2\rho}\frac{\epsilon^2}{k} \quad (8)$$

And the model constants are as below. σk and σε are the turbulent Prandtl numbers for k and ε, respectively. These default values have been determined from experiments with air and water. Navier stokes equations are as follow[17]:

$$\frac{\partial_u}{\partial_x}+\frac{\partial_v}{\partial_y}=0 \quad (9)$$

$$\frac{\partial u}{\partial t}+\mu\frac{\partial v}{\partial x}+v\frac{\partial v}{\partial y} = F_x-\frac{\partial p}{\partial x}+\frac{1}{Re}\left[\frac{\partial^2 u}{\partial x^2}+\frac{\partial^2 u}{\partial y^2}\right] \quad (10)$$

$$\frac{\partial u}{\partial t}+\mu\frac{\partial v}{\partial x}+v\frac{\partial v}{\partial y} = F_x-\frac{\partial p}{\partial y}+\frac{1}{Re}\left[\frac{\partial^2 v}{\partial x^2}+\frac{\partial^2 u}{\partial y^2}\right] \quad (11)$$

3. Design Modeler and Analysis

3.1 Design modeler and material selection

Full size of Filter is 326 × 136 × 10mm, and was composed of a total of 54Cell. backflow can occur due to the flow of the fluid, this is the reason why we modeled the inlet portion and the outlet portion larger. In addition, the shape of the filter is shown in Fig. 1 and deformation angle and length of the six shapes modeled Filter.

Filter for OTR, due to excellent heat resistance and excellent mechanical strength, PPS resin one of the super engineering plastics was selected. PPS was selected as the material for OTR filter by the reason PPS is superior to injection molding, and also when compared with equivalent mechanical properties of the material with the cheaper price.

3.2 Fluid flow analysis

The oil of the size from 1 to 10 in the air in Filter inlet has been flowing at a rate of 1.15m/s, between the incoming oil and oil cannot interact with each other to flow. In addition, escape condition granted in part the inlet and the outlet of filter and the fluid was able to pass through like Fig. 2, granted Reflect the peripheral wall portion was tossed out in the case the fluid touches the wall. If the oil touches each cell of the filter, it can be removed. trap conditions were granted. the flow mesh size is about 1.4mm, each of the nodes and elements are organized into 334,730 dogs and 330,914. By adding refinement conditions, generated mesh to evenly divide size of mesh around filter. The flow analysis was performed until the fluid in the flow field to fully converge.

The physical properties of the air and oil used in the analysis was set as shown like Table 1 The oil was used in the analysis of material used the BIS Phthalate the material.

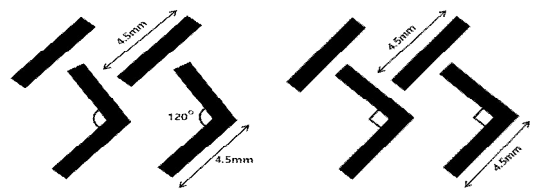

(a) Type 1 **(b) Type 2**

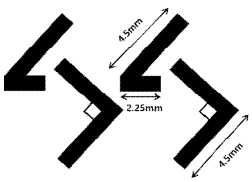

(c) Type 3

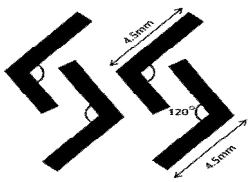

(d) Type 4

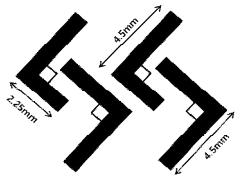

(e) Type 5

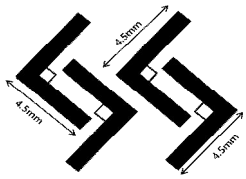

(f) Type 6

Fig. 1 Filter shape of types

Fig. 2 Boundary condition

Table 1 Operating conditions and properties

Fluid	Air-Liquid
Pattern	Dispersed
ρ_1(kg/m3)	980
ρ_g(kg/m3)	1.225
μ_g(kg/m·s)	0.0242
μ_1(kg/m·s)	0.001

4. Results of Numerical Analysis

4.1 The characteristics of surface roughness

Fig. 3 shows the flow of the fluid velocity inside the filter, Fig. 4 is expressed by particle size distribution was detected in each type outlet. all six types of a total of 306,000 particles was entered through the inlet. In the case of the type 1, the number of particle from outlet is 222,649 and shown as the analysis results. it was confirmed that 1 to 10 escaping evenly. In the case of the type 2, the size of the joint angle is 90 degrees and total 91,413 of particles were passed through. It is indicated larger than of 5 or more is 70% or more of the removal efficiency, less than 50% is not been removed not that much and then escaped. In the case of the type 3, the number of particles at the outlet is 62830, more than 5 of particles are removed more than 90%. However, the particle removal efficiency is less than 50% much of the fine particle is not removed and left. The number of particles detected is a total of 213,425 of the type 4 in the outlet. we confirmed that 1 to 10 of them escaped evenly. the case of the type 5, the number of particles detected in the outlet is a total of 90,400, particle less than 5 of them went through a lot. It seemed the high removal rate of particles which is larger than it, but 10 particle was not removed as all did. In the case outlet of the type 6, a total of 51,135 particles were detected. Less than 4 particle went out bet more than 8 particle were removed was found.

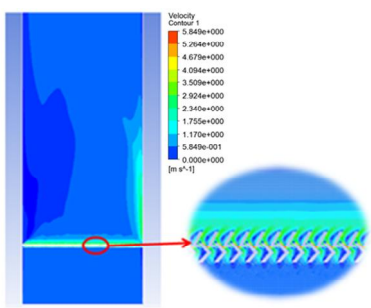

(a) Type 1

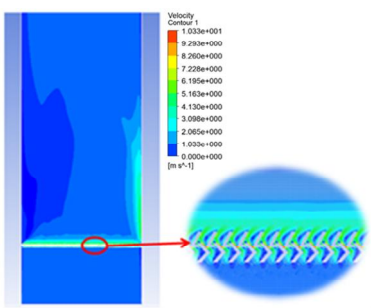

(b) Type 2

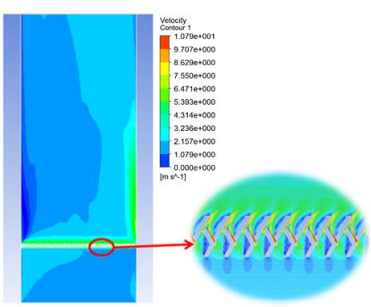

(c) Type 3

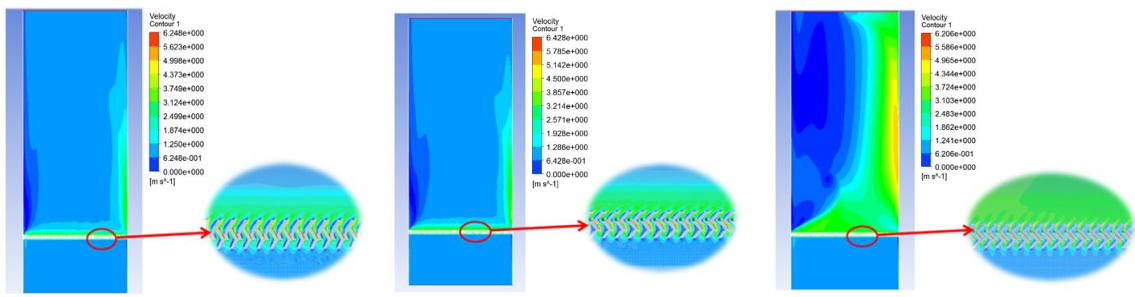

(d) Type 4 (e) Type 5 (f) Type 6

Fig. 3 Velocity distribution of fluid flow

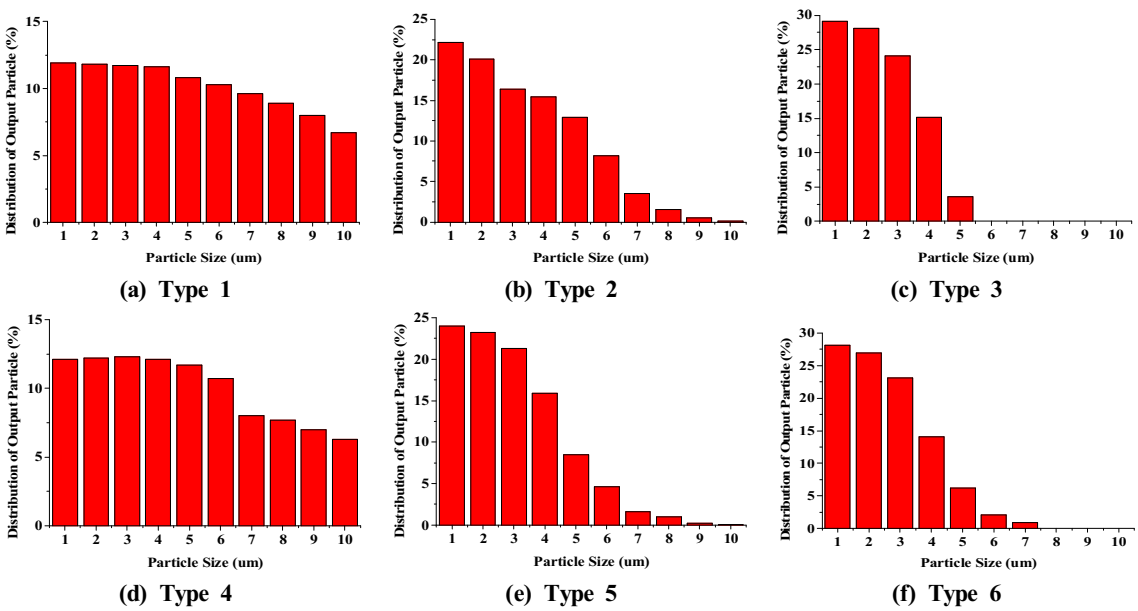

(a) Type 1 (b) Type 2 (c) Type 3

(d) Type 4 (e) Type 5 (f) Type 6

Fig. 4 Distribution of output particle of filters

Fig. 5 and Table 2 show the removal efficiency in each type of the results of the flow analysis performed. There are six types of flow analysis results showed 27.2% removal efficiency of the Oil Mist filter consists of inner angle 120° in the first type. Removal efficiency of small particle size less than 1 is about 15% and most of particle was not being removed by just drained. Removal efficiency of the biggest particle 10 or more is about 50%, it was confirmed most of particle was drained. at this time pressure loss of filter is about 1.6mmAq, Filter shape is simple so removal efficiency is low, but the pressure loss is low.

In second case which consists of 90 degrees of joint angle and removal efficiency of particle is about 70.1%, so removal efficiency was more rapidly increased than joint angle 120 degrees. removal efficiency of less than particle size 1 is low as about 30%, more than 10 are almost removed. The pressure loss of the second type is 6.68mmAq and it is

extremely increased than the first type. It appears to be filter shape, as removal efficiency is increased, as pressure loss is also increased.

In the case of third type, filter efficiency is significantly better as about 80% than existing two types. particle less than 1 is confirmed that removed approximately 40% and 6 or more particle is removed 100%. Pressure loss of third type is considerably higher as 7.4mmAq than existing two types. An analysis results showed 30.2% removal efficiency of the oil mist filter consists of inner angle 120° in the fourth type. In the case oil mist by particle size particle removal efficiency compared to small size 1, less than 20% removal efficiency, showed removal efficiency of about 50% in 10 biggest Particle. Pressure drop of first type is about 1.76mmAq.

We were able to get very good results of the fifth type, consisting of filter inner angle 90 ° which the removal efficiency is approximately 67.8% better than the other types. In the case 1 removal efficiency of oil mist particle by size was about 20% not enough, but more than 4 were 50%, and 9 close to 100% removal was confirmed. The second type of pressure drop was about 2.38mmAq. Lastly, the sixth type consisting of the same length of the each cell filter, inner angle 90°, was very high as 83.2% in the removal efficiency of the oil mist. In addition, particle size removal efficiency was more than 70% in 1 and almost 100% removal was confirmed in 6. The pressure drop showed a slight increase in the degree of pressure drop 3.3mmAq than the earlier two types.

The results of filter flow analysis, filter made of inner angle 90° showed the highest removal efficiency. consisting at 120° filter was better in the pressure drop but even if the pressure drop is higher 3.3mmAq, it is the best to use a third type of filter consisting of 90° in the superior removal efficiency of fine particle removal efficiency.

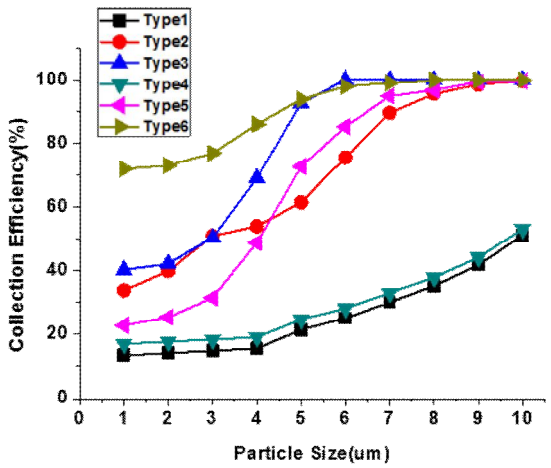

Fig. 5 Collection efficiency according to filter type

Table 2 Concentration efficiency by particle size according to filter type

Efficiency for Particle Size (%)											
Size(um)	1	2	3	4	5	6	7	8	9	10	Avg.
Type1	13.4	14.1	14.8	15.5	21.4	25.1	0.1	35.2	41.1	51.2	27.2
Type2	33.8	39.9	51.1	53.9	61.4	75.5	89.5	95.5	98.5	99.7	69.9
Type3	40.2	42.3	50.5	68.9	92.6	100	100	100	100	100	79.5
Type4	17	17.6	18.3	19	24.6	28.1	33	37.9	44.2	53.2	29.3
Type5	22.8	25.3	31.5	48.8	72.6	85.2	94.8	96.7	99.3	99.6	67.7
Type6	71.9	73	76.9	85.9	93.8	97.9	99.1	100	100	100	89.9

5. Performance Evaluation with Experimental Results

To conduct performance evaluation type 6 model of the Filter with the best results flow, analysis was modeled using a CAD program CATIA V5, 3D printer was constructed using a Rapid Prototyping System. ABS resin was used in the material 3D printer.

Fig. 6 Type 6 filter created with 3D printer

First, the efficiency of performance evaluation experiments evaluated the performance utilizing the equipment in the picture below. Fig. 7, measuring apparatus for measuring the oil mist atomizer, generate a particle filter fan with a constant air flow from 1 to 10 in atomizer, measured from the back side of the particle number. efficiency was calculated by measuring the number of the particle filter with / without.

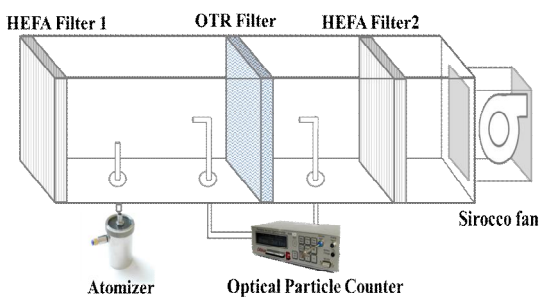

Fig. 7 Experimental equipment for the evaluation of filter performance

Table 3 Efficiency result comparison of analysis and test

Efficiency for Particle Size (%)											
Size(um)	1	2	3	4	5	6	7	8	9	10	Avg.
Analysis	71.9	73	76.9	85.9	93.8	97.9	99.1	100	100	100	89.9
Test	62.5	65	74.6	88.7	91.5	94.5	97.5	98.7	99.9	99.9	87.3

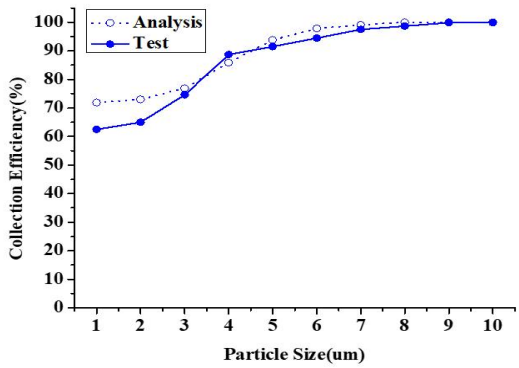

(a) Collection Efficiency

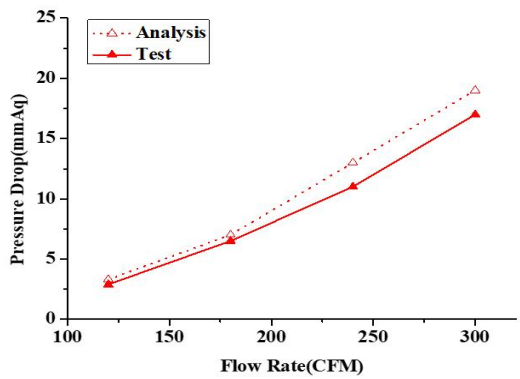

(b) Pressure Drop

Fig. 8 Result comparison of analysis and test(Type 6)

Table 3 and Fig. 8(a) is compared analysis and experimental values of type6 efficiency Type 6 filter efficiency test results slightly reduced with an efficiency of 87.3% and it is almost similar trend and the resulting value. the analysis and experimental values showed error of less than 3%. There is a difference of about 10% in the particle size of 1,2um, but there is almost a match in the size of more than 3um. this analysis, applying between particle without interaction, but less than 2 can occur in real test due to a conflict by interaction in particle. Therefore, it can be less than 2 is considered that the difference.

The pressure drop of type 6 filter measured by airflow rate. air flow rate was set at 120, 180, 240, 300CFM. we received a better result of pressure drop in the actual test than interpretation results, but also

showed a similar trend. the interpretation results of pressure drop test and efficiency were compared with the data shown in Fig. 8(b) and Table 3.

6. Conclusion

In order to improve the performance of microwave hood combination filter, this study is performed by changing the shape of the filter using the program ANSYS13.0 Fluent which is for studying fluent computational fluid dynamics. selected one of the best performance based on the analysis results, produced mock-up using equipment performance evaluation then performance evaluation test was performed.

As a result of the analysis performed by modeling, the three types of Filter, the inner angle 90° has excellent performance rather than an angle of 120°. we believe that the smaller size of inner angle, the higher efficiency we could get. due to the nature of the filter that cannot design with less than 90°, inner angle 90° is the most suitable.

It is also determined that the difference in length of filter was caused, the longer the length of the filter can be attached to the particle filter area is also increased and thereby the difference in efficiency occurs. in type 6 filter the interpretation of the results and compare the results of the efficiency tests, showed error of less than 3%.

When applying the type 6 filter to the OTR filter, the optimum filter can remove more than 87.3% between 1 and 10um of oil mist. in addition, it could contribute to the prevention of environmental pollution by emitting less oil mist outside.

References

1. Phillops, M. J., Smith, E. A., Mosquin, P. L., Chartier, R., Nandasena, S., Bronstein, K., Elledge, M. F., Thornburg, V., Thornburg J., “Sri Lanka Pilot Study to Examine Respiratory Health Effects and Personal PM2.5 Exposures from Cooking Indoors,” Int. J. Environ. Res. Public Health, Vol. 13, No. 791, 2016.
2. Pu, G., Zeng, M., Lu, S., Huang, R., “Study on the Use of Cooking Oil in Chinese Dishes,” Int. J. Environ. Res. Public Health, Vol. 16, No. 3367, 2019.
3. Jeon, W. H., Rew, H. S., Song, S. B., Shon, S. B., “A Study on the Aeroacoustic Characteristics of the Sirocco Fan of Over the Range,” Korean Fluid Machinery Association, Vol. 7, No. 1, pp. 17-23, 2004.
4. Wan, M. P., Wu, C. L., To, G. N. S., Chan, T. C., Chao, C. Y. H., “Ultrafine particles, and PM2.5 generated from cooking in homes,” Atmospheric Environment, Vol. 45, pp. 6141-6148, 2011.
5. Kang, K., Kim, H. K., Kim, D. D; Lee, Y. G., Kim, T. Y., “Characteristics of cooking-generated PM10 and PM2.5 in residential buildings with different cooking and ventilation types,” Science of Total Environment, Vol. 668, pp. 56-66, 2019.
6. Pozorski, J., Apte, S. V., “Filtered particle tracking in isotropic turbulence and stochastic modeling of subgrid-scale dispersion,” Int. J. Multiphase Flow, Vol. 35, pp. 118-128, 2009.
7. Rzehak, R., Kriebitzsch, S., “Multiphase CFD-simulation of bubbly pipe flow: A code comparison,” Int. J. Multiphase Flow, Vol. 68, pp. 135-152, 2015.
8. Guyot, M. K., Ormiston, S. J., Soliman, H. M., “Numerical analysis of two-phase flow from a stratified region through a small circular side branch,” Int. J. Multiphase Flow, Vol. 87, pp. 175-183, 2016.
9. Jeon, W. H., Rew, H. S., Song, S. B., Shon, S. B., “A Study on the Aeroacoustic Characteristics of the Sirocco Fan of Over the Range,” Korean Fluid Machinery Association, Vol. 7, No. 1, pp. 17-23, 2004.

10. Shin, Y.I., “An Experimental Study on the Effective Enhancement for Hood Performance of OTR Microwave Oven,” Master’s Thesis, National Pusan University, Pusan, Korea, 2010.
11. Gharib, J., Moraveji, M. K., “Determination the Factors Affecting the Vane-Plate Demisters Efficiency Using CFD Modeling,” Journal of Chemical Engineering & Process Technology Vol. 1, No. 3, 2012.
12. Ryan, E., Militello, H., Miller, S. L., “The impacts of cooking and an assessment of indoor air quality in Colorado passive and tightly constructed homes,” Building and Environment, Vol. 144, pp. 573-582, 2018.
13. Zhang, J., Pan, W., Long, Z,; Wang, C., Feng, Z., “Study of the Oil Mist Filtration Performance: Pressure Drop Characteristics and Filter Efficiency Model,” Aerosol and Air Quality Research, Vol. 17, pp. 1063-1072, 2017.
14. Wu, X., Liu, L. D., Luo, X. W., Chen, J. W., Dai, J. W., “Study on Flow Field Characteristics of the 90 Rectangular Elbow in the Exhaust Hood of a Uniform Push−Pull Ventilation Device,” Int. J. Environ. Res. Public Health, Vol. 15, No. 2884, 2018.
15. Chen, X., Wheeler, C., “Computational Fluid Dynamics (CFD) modelling of transfer chutes: Assessment of viscosity, drag and turbulence models,” Int. J. Multiphase Flow, Vol. 69, pp. 42-53, 2015.
16. Kim, B.Y. A Study on Indoor Air Cleaning in Crowd Facilities using Arc Reaction: Focused on Bacteria Sterilization from the Air. Ph. D. Thesis, Myongji University, Seoul, Korea, 2011.
17. Mallouppas, G., George, W. K., Wachem, B. G. M. V., “Dissipation and inter-scale transfer in fully coupled particle and fluid motions in homogeneous isotropic forced turbulence,” Int. J. Multiphase Flow, Vol. 67, pp. 74-85, 2017.
18. Kwac, L. K., Kim, H. G., Ko, S. C., Kang, S. S., “The Development of Technology for oil Mist and Odor Removal Using Cab Type Filter,” KSMTE, Vol. 46, pp. 452-455, 2009.